# Phase Transitions in AlAs/GaAs Superlattices under High Pressure

B. A. Weinstein and S. K. Hark
*Xerox Corporation, Webster Research Center, Webster, New York 14580*

and

R. D. Burnham and Richard M. Martin
*Xerox Corporation, Palo Alto Research Center, Palo Alto, California 94304*
(Received 22 October 1986)

Pressure-induced structural transitions in AlAs/GaAs superlattices and in a bulk film of AlAs are reported for the first time. For layers thicker than a few hundred angstroms, the transition occurs in individual AlAs layers, superpressed above the bulk stability limit, with a volume change that destroys the interface coherence. However, for layers thinner than 100 Å the volume change is partially accommodated by formation of a strained-layer superlattice. The stability of strained high-pressure phases is explored with use of density-functional calculations.

PACS numbers: 64.70.Kb, 81.30.Hd

Under pressure, tetrahedral semiconductors undergo strongly first-order transitions to more closely packed structures, with large changes in volume, ~15%–20%. The most common high-pressure phases are sixfold coordinated and tend to be metals or small-band-gap semiconductors.[1-4] In addition, metastable structures can be retained in some materials when pressure is released.[5] These transitions can now be understood theoretically by use of *ab initio* density-functional methods.[6,7]

Whereas previous work has dealt with pressure-induced structural transitions in bulk solids,[1-4] our present studies are concerned with how these transitions are modified in crystalline superlattices. We treat the lattice-matched AlAs/GaAs system. This system is a candidate for new effects not present in any homogeneous material as a consequence of the different transition pressures of its bulk constituents. These pressures are $P_t^G = 172$ kbar for GaAs (to a distorted NaCl structure[4]) versus $P_t^A = 123$ kbar for AlAs (structure unknown) as established for the *first time* by our work. For example, it has been shown that the zinc-blende phase of AlAs can be superpressed far above $P_t^A$ by the constraint of lattice matching to GaAs.[8] Here, we consider from the standpoint of experiment and theory the energetics of two types of transitions within the layers of superlattices.

Visible microscopy was used to detect the transformation of thin layers to opaque states. This was quite unambiguous because the samples became transparent prior to any phase transitions as a result of the pressure-induced increase of the GaAs band gap.[9] We studied four types of samples (respectively numbered 1–4 in Table I)—bulk GaAs, a single "bulk" film of AlAs (1.1 μm thick) imbedded in GaAs, and two AlAs/GaAs superlattices with different layer thicknesses. All (except bulk GaAs) were grown by metalorganic chemical vapor deposition, with (001) orientation, and without intentional doping. The superlattices were processed with a GaAs-selective etch[10] to obtain free-standing epilayers. Hydrostatic pressure ($P$) was applied at room temperature with a diamond-anvil cell.[11] Luminescence from the samples was monitored to check for transition-induced defects.

The observed phase transition in bulk GaAs (sample 1) conformed to previous results,[2,4] exhibiting its threshold at 172 kbar, sluggish nucleation kinetics, and irreversibility. The latter implies retention of a metastable phase at $P = 0$.[2]

The geometry of sample 2, a macroscopic AlAs layer protected from oxidation by thick GaAs layers (Table I), allowed us to establish the transition pressure of AlAs in essentially bulk form. Since this threshold, $P_t^A = 123$ kbar, was too low for the adjacent GaAs layers to transform, the bond coherence at the two AlAs-GaAs interfaces was broken during the transition. This deduction is reinforced further, below. In contrast to bulk GaAs, the

TABLE I. Sample characteristics and transition pressures.

| Sample | Morphology | $P_t$ (kbar) | $R_t$ (kbar) |
|---|---|---|---|
| 1 | Bulk GaAs<br>~20 μm<br>1 cycle | 172 ± 4 | No reversal |
| 2 | GaAs/AlAs/GaAs<br>0.3/1.1/0.3 μm<br>1 cycle | 123 ± 4 | 60 ± 10 |
| 3 | AlAs/GaAs<br>290/160 Å<br>60 cycles | 142 ± 4 | 70 ± 10 |
| 4 | AlAs/GaAs<br>60/25 Å<br>200 cycles | 166 ± 4 | 115 ± 10 |

AlAs transition was reversible. When $P$ was lowered from $P_t^A$, sample 2 reverted to a transparent state at 60 kbar. However, the color was somewhat darker than originally, probably as a result of below-band-gap absorption by transition-induced microscopic defects.

Figure 1 documents the phase changes of both superlattice samples within the same pressure environment. In our discussion, the thresholds for the first and second increasing-pressure transitions in *each* superlattice will be denoted $P_t^{(1)}$ and $P_t^{(2)}$, respectively. A key factor affecting $P_t^{(1)}$ turns out to be the AlAs layer thickness $l$, which is 290 and 60 Å in samples 3 and 4, respectively (Table I). Sample 3 transformed at $P_t^{(1)}=142$ kbar in the following remarkable manner. Just below $P_t^{(1)}$ the sample was yellow and clear, similar to sample 4 in Fig. 1(a). At $P_t^{(1)}$ there was a sudden change to a darker but *still transparent* color; the process took $<0.1$ sec and was uniform across the sample. In quick succession, six similar changes were observed, separated by $\sim 15$-sec intervals, until the superlattice was completely opaque as shown in Fig. 1(a). We conclude that these transitions involved only the AlAs layers. If GaAs layers also transformed, there would be no isolation between layers, and the entire transformation would have occurred in one continuous process instead of in discrete steps. Given that seven steps were needed to produce opacity, it is likely that transitions in individual AlAs layers were observed ($7\times 290$ Å $\approx 2000$ Å, a typical metallic penetration depth). A corollary result is that large numbers of defects were formed at each AlAs-GaAs interface, thereby destroying the interface coherence and producing the requisite layer isolation.

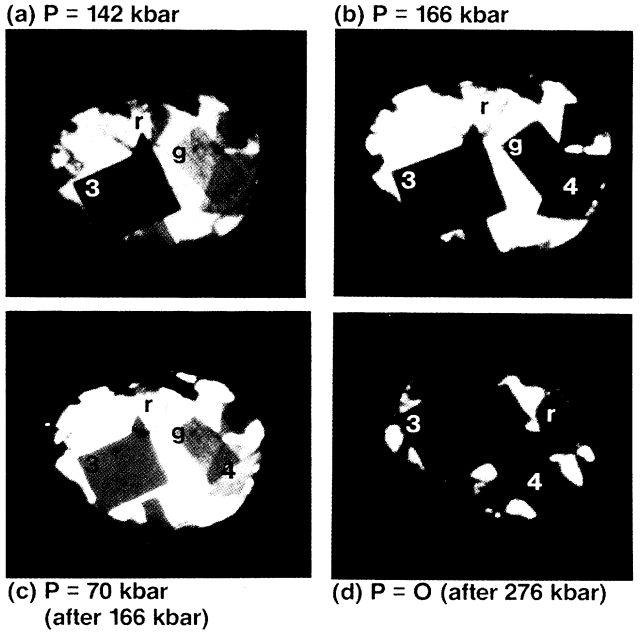


FIG. 1. Photographs showing several chips of two different AlAs/GaAs superlattices, and ruby (labeled $r$), inside the diamond-anvil cell. Samples are numbered according to Table I. All are free floating, except 4g, which was attached to one anvil face with $\sim 10$ $\mu$m of light grease (Ref. 12). (a) $P=142$ kbar. Only sample 3 transforms at this pressure, 19 kbar *above* the bulk AlAs transition. (b) $P=166$ kbar. Both superlattices have now transformed, still 7 kbar *below* the bulk GaAs transition. (c) $P=70$ kbar, reduced from 166 kbar. All superlattices regained transparency. (d) $P=0$, reduced from 276 kbar. No samples retransform.

Sample 4 (free floating[12]) did not transform until $P_t^{(1)}=166$ kbar [Fig. 1(b)]. The transformation was qualitatively different from that in sample 3—in fact, more typical of bulk semiconductors. Discrete individual-layer transitions were not observed, but instead several dark nucleation centers appeared and grew, in both size and opacity, until after $\sim 15$ min the specimen was completely black. It is difficult to decide here whether the entire superlattice, AlAs and GaAs layers, transformed as a monolithic bulk solid, or whether only the AlAs component transformed. However, the pressure-cycling results presented below support the *latter* possibility.

Cycling the pressure over the range 0–276 kbar had the following outcome. Samples 3, 4, and 4g each retransformed to a transparent state if $P$ was reduced from equal to or slightly above $P_t^{(1)}$ [Fig. 1(c)]. This reversal was essentially a backward replay of the corresponding increasing-pressure transition, except that the thresholds $R_t$ were some 50–70 kbar below $P_t^{(1)}$ (Table I). In contrast, if $P$ was reduced from a maximum much greater than $P_t^{(1)}$, retransformation did not occur [Fig. 1(d)]. The latter case is indirect evidence for a second phase change at higher pressure. It probably occurs in the GaAs layers, which are expected to transform at a pressure $P_t^{(2)}\leq P_t^G$. With the zinc-blende template provided by the GaAs layers now lost, the reverse transition would be inhibited, resulting, just as for bulk GaAs,[2] in an opaque metastable phase after pressure release. For sample 4 (also 4g), the existence of such a transition in the GaAs layers implies that the phase change at $P_t^{(1)}$ involved only the AlAs layers, as was proposed above.

The condition of the retransformed superlattices has important consequences. No new cracks or blemishes were apparent [Fig. 1(c)] in any of the specimens. However, samples 3 and 4g were darker in color, and none of the superlattices any longer emitted luminescence (even at $P=0$), whereas initially all exhibited strong emission until their band gaps became indirect above $\sim 40$ kbar.[9] Hence, although the transitions appeared macroscopically uniform, they produced enough microscopic defects to cause below-band-gap absorption and luminescence quenching. Moreover, the *unchanged color* of the free-floating sample 4 implies that (in the absence of strain gradients) fewer defects were formed in this superlattice compared to sample 3. This supports the idea that high numbers of interface defects were created during the individual-layer transitions in sample 3. Consequently,

we expect the interface bond coherence in sample 4, the *thinner-layer* superlattice, to be better preserved.

The observed superpressing that raises $P_t^{(1)}$ above $P_t^A$ for AlAs layers in AlAs/GaAs superlattices can be attributed to an energy barrier against transformation caused by the initial interface constraint of bond registry to GaAs. We can estimate this barrier from the extra work done by pressure to transform AlAs layers within a superlattice over that required to transform bulk AlAs. This is found by evaluation of

$$\Delta E = -\int_{P_t^A}^{P_t^{(1)}} PdV - P_t^{(1)}\Delta V_t^{(1)} + P_t^A \Delta V_t^A.$$

Approximate values can be obtained by our taking both $\Delta V_t^A$ and $\Delta V_t^{(1)}$, the transition volume changes in AlAs at $P_t^A$ and $P_t^{(1)}$, to be $-17\%$ (equal to $\Delta V_t^G$ in bulk GaAs[4]), and using Murnaghan's equation of state[6] to integrate $-PdV$. We neglect the slight change in lattice matching prior to the transition. The result for samples 2–4, normalized to the $P=0$ volume $V_0$, is plotted in Fig. 2 (points) as a function of the reciprocal AlAs layer width $1/l$.

In our interpretation, $\Delta E/V_0$ is subject to two limits set by the solid lines in Fig. 2. The first is an upper bound that corresponds to $P_t^{(1)} \rightarrow P_t^G$. Above this the GaAs will transform and will no longer hinder the transition in AlAs. The second limit applies for thick AlAs layers. In that case, $\Delta E/V_0$ is expected to arise from the formation of interface defects, and hence, to scale as $1/l$—viz., a constant defect energy per unit area, $\Delta E/\sigma_0$, averaged over $l$. From the slope of the asymptote intersecting the origin in Fig. 2, we estimate $\Delta E/\sigma_0 \sim 0.9$ eV/Å$^2$. This corresponds to roughly three broken AlAs bonds (1.89 eV each[13]) per atom in a (100) plane at each interface, suggesting that the region of interface defects extends over several monolayers.

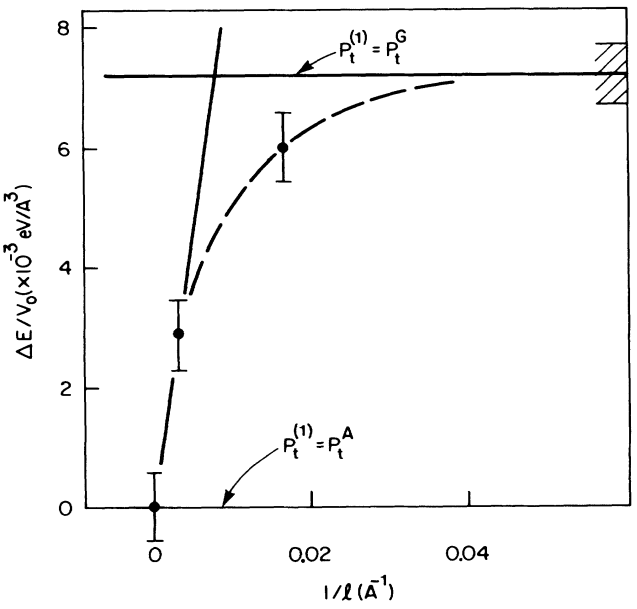


FIG. 2. Energy barrier $\Delta E/V_0$ described in text vs the reciprocal AlAs-layer thickness $1/l$. Data points correspond to samples 2–4; error bars represent $\pm 4$-kbar uncertainty in the measured threshold pressure. Asymptote intersecting origin defines the interface-defects limit. Horizontal asymptote is the upper limit set by the bulk GaAs transition. Dashed curve depicts hypothetical path spanning these limits for a strain-defect admixture appropriate to sample 4.

Note that $\Delta E/V_0$ for sample 4 lies below the $1/l$ asymptote. We believe that this results from the increasing ability of a thin-layer superlattice to accommodate the $\sim 15\%$–$17\%$ volume decrease in the AlAs layers by transforming to a strained-layer system. In that case $\Delta E/V_0$ would be determined by the extra energy to produce the strain. If elastic continuum theory is applicable, this is expected to vary as the square of the interface-parallel strain, saturating for vanishing $l$ as $A(1+Bl)^{-2}$, with $A$ and $B$ constants involving the linear misfit, shear moduli, and GaAs layer width.[14]

A rough criterion, often applied to as-grown strained-layer superlattices, can be used here to estimate the critical layer thickness $\lambda_c$ below which strained layers are more favorable than misfit defects.[14] It is $\lambda_c \approx (b/4f) \times [\ln(\lambda_c/b)+1]$, where $b$ is the dislocation strength, typically $\sim 4$ Å, and on the basis of $\Delta V_t$, we take the linear misfit $f$ to be 3%–5%. This gives $\lambda_c \sim 100$ Å, indicating that a strained-layer structure is appropriate for the high-$P$ phase of sample 4. However, for real superlattices there should be a substantial range of $l$ exhibiting intermediate behavior. After a transition, an interface would then be characterized by defect clusters at some regions and varying degrees of strain at others; we think that this situation applies to sample 4.

Although at present the crystal structure of the transformed superlattice layers is undetermined, it is instructive to explore the nature of transitions in hypothetical structures with use of total energy theory. Here we report results which show that the microscopically calculated strain energies are consistent with our previous conclusions. Additional results are presented elsewhere.[8] We have used *ab initio* pseudopotential density-functional methods described previously,[7] with a plane-wave basis up to 18 Ry. Figure 3 shows calculated curves giving the enthalpy $H=E+PV$ of AlAs and GaAs in their respective NaCl structures relative to the enthalpy in their respective zinc-blende structures. Transitions are predicted to occur where the curves cross $H=0$; for the bulk materials (solid lines) this yields pressures of 90 kbar for AlAs and 170 kbar for GaAs, in reasonable agreement with experiment[4] and previous theory.[6]

The dashed curve in Fig. 3 is for transformed AlAs (NaCl structure) strained to match untransformed GaAs (zinc blende) at a (111) interface. For simplicity, we fix the GaAs lattice spacing at 5.4 Å ($\sim 135$ kbar) and vary only the AlAs layer-normal spacing. This is a represen-

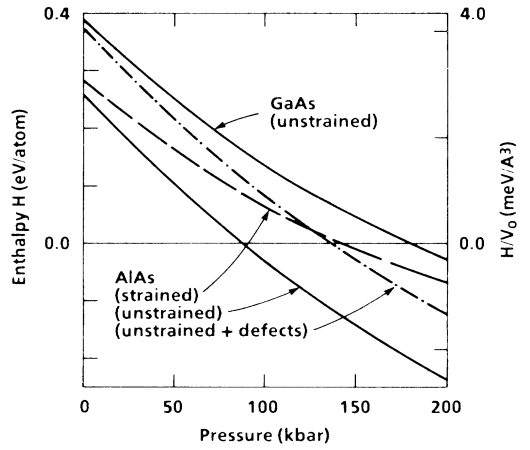


FIG. 3. Enthalpy $H=E+PV$ of AlAs and GaAs in their respective NaCl structures referred to that in their respective zinc-blende structures. Transitions occur at the abscissa crossings. The dashed curve shows the effect of strain for transformed AlAs constrained to match untransformed (i.e., zinc-blende) GaAs. Dash-dotted curve is representative of the interface-defects limit.

tative example; the strain energies would be larger for a (100) interface, but smaller if sharing of strain between the AlAs and the GaAs was included. The dash-dotted curve in Fig. 3 simulates the interface-defects limit. This is obtained from the unstrained AlAs curve by a constant increase in enthalpy proportional to $1/l$. It is clear from Fig. 3 that, as $l$ decreases, defects will be favored over strain until the crossing of their respective curves at $H=0$. After this crossing, the energy of the transformed superlattice can be reduced by a strained geometry, but, as noted above, a strain-defect admixture is more realistic. We expect the latter to yield a dependence of $\Delta E/V_0$ on decreasing $l$ that resembles the hypothetical dashed curve in Fig. 2, with the exact variation determined by the particular admixture. Thus, the calculations summarized in Fig. 3 exhibit the correct qualitative behavior.

In conclusion, our observations of superpressing, individual-layer transitions, and reversibility indicate that superlattice transitions can be strongly influenced by the competition between formation of interface defects and that of strained layers in the high-pressure phase. Future studies should include high-pressure Raman, x-ray, and extended x-ray-absorption fine-structure measurements to determine in detail the crystal structure and strain state of transformed layers.

We thank C. Mailhiot for many informative discussions and D. Cobb for his skillful photography.

[1]J. C. Jamieson, Science **139**, 762, 845 (1963).

[2]S. C. Yu and I. L. Spain, Solid State Commun. **25**, 49 (1978); J. Sites and I. Spain, private communication.

[3]S. Minomura and H. G. Drickamer, J. Phys. Chem. Solids **23**, 451 (1962).

[4]M. Baublitz, Jr., and A. L. Ruoff, J. Appl. Phys. **53**, 6179 (1982).

[5]J. S. Kasper and S. M. Richards, Acta Crystollogr. **17**, 752 (1964).

[6]S. Froyen and M. L. Cohen, Phys. Rev. B **28**, 3258 (1983).

[7]R. Biswas, R. M. Martin, R. J. Needs, and O. H. Nielsen, Phys. Rev. B **30**, 3210 (1984).

[8]B. A. Weinstein, S. K. Hark, and R. D. Burnham, in Proceedings of the Eighteenth International Conference on the Physics of Semiconductors, Stockholm, Sweden, 1986 (to be published); R. M. Martin, *ibid.*, and to be published.

[9]R. Zallen and W. Paul, Phys. Rev. **155**, 703 (1967); B. A. Weinstein, S. K. Hark, and R. D. Burnham, J. Appl. Phys. **58**, 4662 (1985).

[10]R. A. Logan and F. K. Reinhart, J. Appl. Phys. **44**, 4172 (1973).

[11]G. J. Piermarini and S. Block, Rev. Sci. Instrum. **46**, 973 (1975).

[12]The potential effect of nonhydrostatic strain on the transition thresholds was gauged by comparison of the behavior of samples 4 and 4g (Fig. 1). The transition in sample 4g began at 156 kbar but did not go to completion until $P$ was raised to 160 kbar as a result of local strain gradients from the grease used to mount this specimen.

[13]W. A. Harrison, *Electronic Structure and the Properties of Solids* (W. H. Freeman, San Francisco, 1980), p. 176.

[14]J. W. Matthews and A. E. Blakeslee, J. Vac. Sci. Technol. **14**, 989 (1977), and J. Cryst. Growth **27**, 118 (1974).

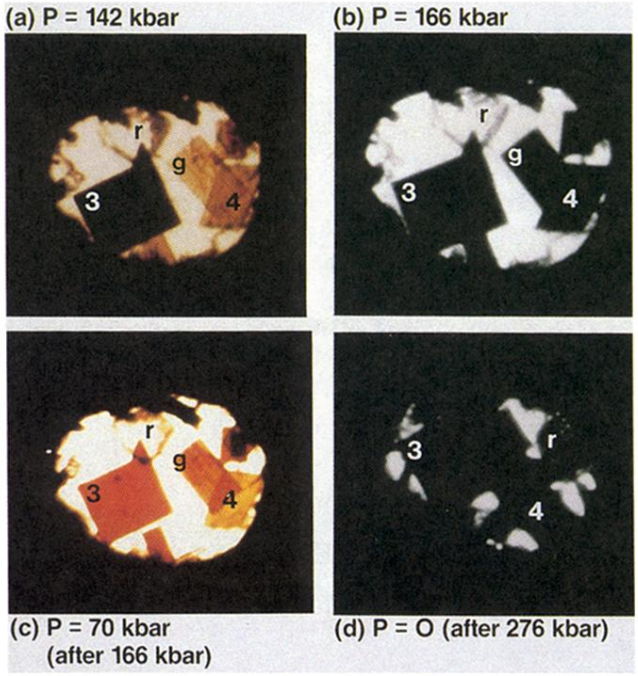


FIG. 1. Photographs showing several chips of two different AlAs/GaAs superlattices, and ruby (labeled *r*), inside the diamond-anvil cell. Samples are numbered according to Table I. All are free floating, except 4g, which was attached to one anvil face with $\sim 10\ \mu$m of light grease (Ref. 12). (a) $P = 142$ kbar. Only sample 3 transforms at this pressure, 19 kbar *above* the bulk AlAs transition. (b) $P = 166$ kbar. Both superlattices have now transformed, still 7 kbar *below* the bulk GaAs transition. (c) $P = 70$ kbar, reduced from 166 kbar. All superlattices regained transparency. (d) $P = 0$, reduced from 276 kbar. No samples retransform.